

TRIUMF	UNIVERSITY OF ALBERTA EDMONTON, ALBERTA	
	Date 1997/11/20	File No. TRI-DNA-97-4
Author GM Stinson		Page 1 of 19
Subject The effect of windows upstream of the target on the beam size at the beam line 2A target		

1. Introduction

A previous note¹⁾ discussed the effect on the beam spot at the west target of beam line 2A of a window placed at various distances upstream of the target. Since that report was issued a decision to insert two windows upstream of the target has been made.

The first, located 44 inches (1.1176 m) upstream of the target, is an aluminum window 0.005 in. thick that serves to isolate the beam line 2A vacuum (and thus the cyclotron) from the (relatively) poor vacuum of the target module. The second, located 16 inches (0.4064 m) upstream of the target, is a copper window 0.010 in. thick at the entrance of the target module containment vessel. (A third window, similar to the second, is located at the exit of the containment vessel but does not concern the study presented here.)

This note presents a REVMOC study of the effect of the effect of these windows on the beam size at the target location.

2. Method of approach

A TRANSPORT²⁾ run was made in which the measured effective lengths of the quadrupoles were used in the determination of the optics of the beam line. In addition the effective length of the 15° dipole that has been field-mapped to date was used for each of the 15° dipoles that direct beam to the target. Because neither of the 27.5° vault dipoles have yet been field-mapped, their effective lengths were taken as the nominal design value.

The effect of these (relatively minor) changes in the effective lengths of the quadrupoles and the 15° dipoles in the TRANSPORT calculations was virtually transparent. Consequently, it is expected that insertion of the measured effective lengths of the remaining 15° dipole and the two 27.5° vault dipoles will not affect the calculations that follow.

Transport element settings obtained from TRANSPORT were inserted into the program REVMOC³⁾ and used to predict the effect of the stripper and the windows on the beam spot at the west target. This was done in three consecutive runs; first, the stripper foil only, second, the stripper foil and the aluminum window and third, the stripper foil and both of the windows. In this manner it was possible to determine which scattering elements most affected the beam size at the target.

In each case 150,000 particles were traced through the system. Each window was divided into the appropriate number of 0.001 in.-thick slices.

2.1 The effect of the stripper foil only

The first run was made with only the stripper foil inserted. This we use as the reference for the beam size at the target. Figure 1 shows the predicted beam size at the west target *without* the stripper foil—that is, what the beam spot is to be predicted to be without foil scattering. In figure 2 is shown the effect on the beam profile when scattering in the foil is included. In these and all subsequent plots, units along the horizontal and vertical axes are cm, the *x*-axis is horizontal and the *y*-axis is vertical.

With no foil scattering REVMOC predicts that the beam size at the target would be ± 0.23 cm horizontally by ± 0.30 cm vertically. When foil scattering is included it is predicted that the beam size will increase to ± 0.32 cm both horizontally and vertically. However, the fraction of beam predicted to lie outside the un-

scattered dimensions of ± 0.23 cm horizontally by ± 0.30 cm vertically is only 0.049% in the horizontal plane and 0.001% in the vertical.

Thus we conclude that foil scattering alone does not contribute substantially to an increase in beam size at the target.

2.2 The effect of the stripper foil and the aluminum window

As a second step, an aluminum window 0.005 in. thick was inserted 44 inches upstream of the target. This window was in addition to the stripper foil. A REVMOC run was then made with this configuration. Figure 3 shows the prediction of the beam size at the west target with scattering in both the stripper foil and the aluminum window included. From figure 3 it is seen that virtually all of the beam is predicted to lie within ± 0.93 cm in each of the horizontal and vertical planes.

The same data, plotted on an expanded scale to match that of figure 2, is shown in figure 4. From figure 4 it is seen that the central core of the beam—that is, that portion lying between ± 0.32 cm in each of the horizontal and vertical planes—contains 99.55% of the beam in the horizontal plane and 99.30% in the vertical plane. Thus the percentage of beam lying outside of the region predicted for the stripper foil only is increased by approximately 0.5% when the 0.005 in.-thick aluminum window is added.

Thus we conclude that the addition of the 0.005 in.-thick aluminum window causes a small additional amount of beam halo but does not significantly disrupt the core of the beam. The vertical size of the beam at the target is predicted to be more affected by scattering in the aluminum window than is the horizontal beam size.

2.3 The effect of the stripper foil and aluminum and copper windows

A final REVMOC run was made with the insertion of a copper window 0.010 in. thick, located 16 inches upstream of the target. The stripper foil and the 0.005 in.-thick aluminum window were also included in this run. Figure 5 is the REVMOC prediction of the beam spot at the west target under these conditions. It is seen that the beam is predicted to fill the entire 4-inch diameter of the beam line at the target location.

The data shown in figure 5 is replotted on an expanded scale in figure 6 where it is seen that REVMOC predicts that only 0.10% of the beam is outside the region bounded by $x = \pm 1$ cm and 0.11% lies outside the region bounded by $y = \pm 1$ cm. Thus approximately 99.8% of the beam is contained in an area of 1 cm^2 .

Figure 7, drawn to the same scale as figure 2, is a plot of the same data on and even more expanded scale. From this figure it is seen that 2.57% of the beam is predicted to lie outside of the region bounded by $x = \pm 0.32$ cm and 3.39% lies outside the region bounded by $y = \pm 0.32$ cm. Thus approximately 94% of the beam lies within the area predicted were the only scatterer the stripper foil.

From figures 5, 6 and 7 we see that the beam is predicted to be significantly larger at the target with the addition of the copper window. Thus we conclude that the addition of the copper window significantly increases beam halo at the target but that approximately 94% of the beam still lies within an area defined by the reference beam ($x = \pm 0.32$ cm and $y = \pm 0.32$ cm).

3. Beam loss and spill calculations

Inherent in the program REVMOC is the calculation of beam loss caused by multiple scattering, absorption and nuclear scattering in materials placed in the beam path. Absorbed particles are removed by nuclear interactions and do not contribute to beam spill downstream. Particles lost by nuclear scattering have been scattered such that they hit the wall of the beam tube causing beam spill and activation of the beam line and its components.

Absorbtion and nuclear scattering data from the above runs are listed in table 1. Losses are tabulated as a function of the distances downstream of the scatterers. Downstream of a scatterer any losses listed at a given point are to be construed as occurring between that point and the previous listed location.

It should be noted that the data presented in table 1 are not inconsistent even though they appear to be. Thus, for example, 0.005% of 150,000 particles represent only 7.5 particles and, given that this is a statistical process, the error on that number is $\pm\sqrt{7.5} = \pm2.74$ or $\pm0.0018\%$. All data presented in the table should be viewed with that in mind.

From table 1 we note that between the vault exit and the aluminum window that separates the beam-line vacuum from the target containment vacuum REVMOC predicts no beam loss—at least to the level of 1 particle in 150,000 or $7 \times 10^{-4}\%$. Beam spill between the exit of the aluminum window and the entrance face of the copper window is predicted to be 0.0159% where we have averaged the predictions for the stripper and aluminum window alone and those for the stripper and aluminum and copper windows. At 100 μA this represents a spill of 15.9 nA per 0.7112 m or 22.4 nA/m. The prediction of beam spill between the exit face of the copper window and the target is 0.0240% over a distance of 0.4064 m (16 in.). Again, at 100 μA this represents a spill of 59 nA/m.

Any designs for target protection and/or beam collimation should bear these figures in mind. To this end we present in figures 8–12 the REVMOC predictions of the beam sizes at and downstream of the aluminum window. Figure 8 shows the beam spot at the exit of the aluminum window where the overall beam size is predicted to be approximately 1.24 cm in the x -plane by 2.5 cm in the y -plane. Figures 9 and 10 show the predicted beam size 0.2794 m (11 in.) and 0.5588 m (22 in.), respectively, downstream of the aluminum window. Figure 11 shows the predicted beam size at the upstream face of the copper window, 0.7112 m (28 in.) downstream of the aluminum window and 0.4064 m (16 in.) upstream of the target. There the beam size is predicted to measure approximately 1.2 cm in each of the horizontal and vertical planes. Finally, figure 12 shows the predicted beam profile 0.1270 m (5 in.) downstream of the copper window.

4. Estimate of power loss in the aluminum and copper windows

Figure 13 shows the same data as figure 8 but on an expanded vertical scale because it is clear from figure 8 that most of the beam at the exit of the aluminum window is contained in an area smaller than 1.24 cm square. From figure 13 we find that 85.8% of the beam lies between $x = \pm0.18$ cm in the horizontal plane and that 87.6% of the beam lies between the same vertical limits (that is, $y = \pm0.18$ cm). On the assumption that horizontal and vertical losses are independent we then have the probability of the beam lying *outside* of an area 0.36 cm square is

$$\begin{aligned} P(\text{outside } x = \pm0.18 \text{ cm and } y = \pm0.18 \text{ cm}) &= P(\text{outside } x = \pm0.18 \text{ cm}) + P(\text{outside } y = \pm0.18 \text{ cm}) \\ &\quad - P(\text{outside } x = \pm0.18 \text{ cm}) \times P(\text{outside } y = \pm0.18 \text{ cm}) \\ &= 0.146 + 0.124 - (0.146)(0.124) \\ &= 0.252. \end{aligned}$$

From this we conclude that 25.2% of the beam lies outside an area 0.36 cm square of that 74.8% of the beam is contained within that area. REVMOC predicts an average energy loss of 1.5×10^{-2} MeV per 0.001 in. of thickness of the aluminum window. Thus a total energy of 0.075 MeV is predicted to be deposited in an area 0.36 cm by 0.36 cm. At a beam current of 100 μA this represents a power density of

$$\begin{aligned} \text{Power density in aluminum window} &= \frac{(0.075 \text{ MeV})(100 \mu\text{A})}{(0.36 \text{ cm})(0.36 \text{ cm})} \\ &= 57.9 \text{ W/cm}^2. \end{aligned}$$

In figure 14 we show the predicted beam profile at the exit of the copper window. Here 93.6% of the beam is predicted to lie between $x = \pm 0.18$ cm and 88.4% of the beam is predicted to lie between the same vertical limits. (Remember that the beam is still converging to the target despite scattering upstream.) Proceeding again on the assumption that horizontal and vertical beam losses are independent we find the probability of the beam lying *outside* of an area 0.36 cm square is

$$\begin{aligned} P(\text{outside } x = \pm 0.18 \text{ cm and } y = \pm 0.18 \text{ cm}) &= P(\text{outside } x = \pm 0.18 \text{ cm}) + P(\text{outside } y = \pm 0.18 \text{ cm}) \\ &\quad - P(\text{outside } x = \pm 0.18 \text{ cm}) \times P(\text{outside } y = \pm 0.18 \text{ cm}) \\ &= 0.064 + 0.116 - (0.064)(0.116) \\ &= 0.173. \end{aligned}$$

Thus 17.3% of the beam is predicted to lie outside of an area 0.36 cm square and therefore 82.7% of the beam lies within that area. For the copper window REVMOC predicts an average energy loss of 4.32×10^{-2} MeV per 0.001 in. of thickness of copper or a total energy deposition of 0.432 MeV. At a beam current of 100 μA the power density that is predicted to be deposited in the window is then

$$\begin{aligned} \text{Power density in copper window} &= \frac{(0.432 \text{ MeV})(100 \mu\text{A})}{(0.36 \text{ cm})(0.36 \text{ cm})} \\ &= 333.3 \text{ W/cm}^2. \end{aligned}$$

To be on the safe side, we suggest that the aluminum window be cooled such that a power density of at least 100 W/cm² could easily be accommodated. For the copper window a cooling capability of at least 600 W/cm² should be designed in.

5. Discussion

This note has presented a study of the effect of the proposed windows that are to be inserted upstream of the west target of ISAC. It is shown that at a beam current of 100 μA the insertion of the aluminum window can be expected to cause beam spills of the order of 20 nA/m downstream of it and upstream of the copper window. The addition of the copper window could produce spills of the order of 60 nA/m between it and the target.

In addition, we suggest that the aluminum window be provided with a cooling capacity of at least 100 W/cm² and that the copper window be provided a cooling capacity of at least 600 W/cm².

References

1. G. M. Stinson, TRIUMF report TRI-DNA-96-8, September, 1996.
2. K. L. Brown and S. K. Howry, *TRANSPORT/360*, SLAC-91, Stanford Linear Accelerator Laboratory, July, 1970.
3. C. J. Kost and P. A. Reeve, TRIUMF report TRI-DN-82-28, TRIUMF, 1982.

Table 1

Calculated beam loss for the cases of
 a) stripper foil only,
 b) stripper foil and aluminum window and
 c) stripper foil and aluminum and copper windows.

All losses are expressed as a percentage of initial beam.

Location	Case a)			Case b)			Case c)		
	Absorbed	Nuclear	Scattered	Absorbed	Nuclear	Scattered	Absorbed	Nuclear	Scattered
Stripper	0.0044			0.0057			0.0078		
Extraction		0.0023			0.0030			0.0042	
Al window				0.0339			0.0382		
Al Window + 0.2794 m					0.0014			0.0008	
Al Window + 0.5588 m					0.0097			0.0130	
Al Window + 0.7112 m					0.0036			0.0033	
Cu window							0.1893		
Cu Window + 0.1270 m					0.0014			0.0025	
West target (Cu Window + 0.4064 m)					0.0031			0.0215	

97/11/18 - 2A AT 500 MEV - FINAL Leff - Stripper ONLY, NO Windows

Space # 8: Distribution of particles as a function of X AT TGT2 (Element #170) (along HORIZONTAL axis)
& Y at TGT2 (Element #170) (along VERTICAL axis)

Distribution of particles INITIALLY ACCEPTED

COUNTS = 150000.
X PROJECTION

1	1	1	1	1	1	1							
1	3	4	4	3	3	1	9	7	5	3	1		
5	2	2	4	9	1	7	8	6	4	3	6		
9	5	1	0	6	4	7	0	9	2	7	5		
0	4	9	3	6	9	7	2	9	7	2	8		

Figure 1. The predicted beam spot at a target *without* foil scattering.

97/11/18 - 2A AT 500 MEV - FINAL Leff - Stripper ONLY, NO Windows

Space # 8: Distribution of particles as a function of X AT TGT2 (Element #169) (along HORIZONTAL axis)
 & Y at TGT2 (Element #169) (along VERTICAL axis)

REAL! Distribution of FINAL RUN FOUND HERE

COUNTS = 149990.
 X PROJECTION

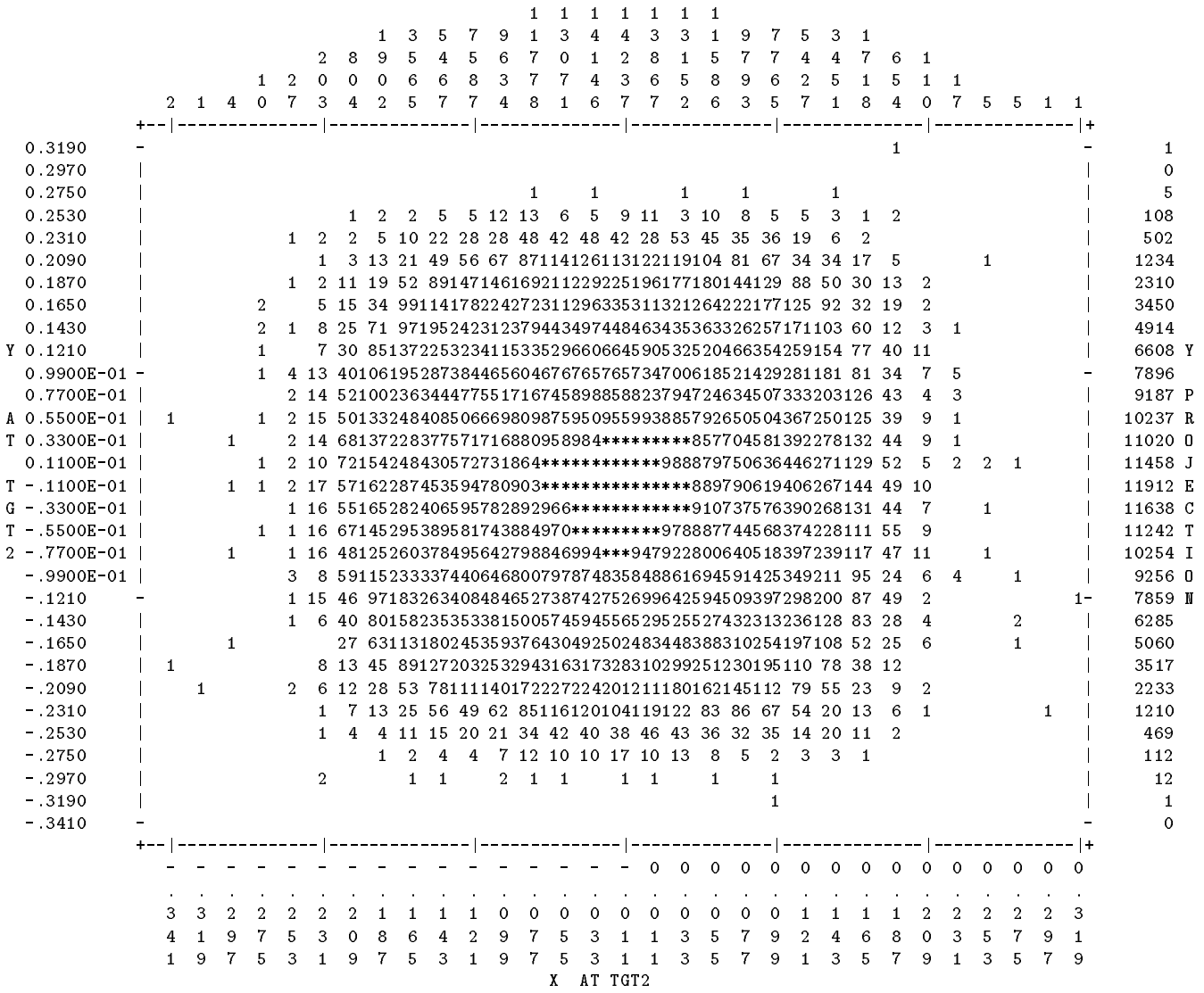


Figure 2. The predicted beam spot at a target *with* foil scattering.

97/11/18 - 2A AT 500 MEV - FINAL Leff - 0.005" Al 44" UPSTREAM of target

Space # 7: Distribution of particles as a function of X AT TGT2 (Element #169) (along HORIZONTAL axis)
 & Y at TGT2 (Element #169) (along VERTICAL axis)

REAL! Distribution of FINAL RUN FOUND HERE

COUNTS = 149907.
 X PROJECTION

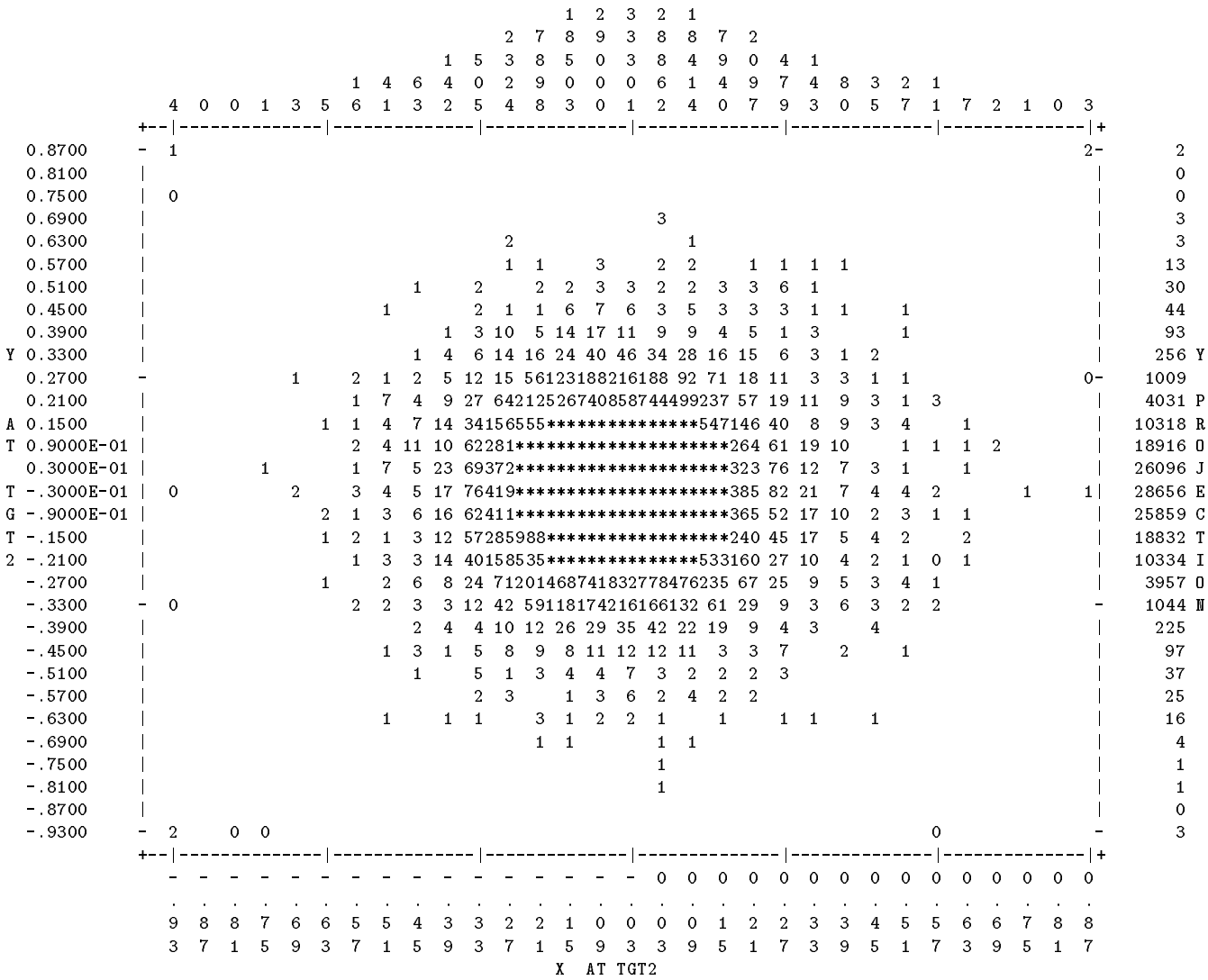


Figure 3. The predicted beam spot at the target with scattering from the foil and 0.005 in.-thick aluminum window.

97/11/18 - 2A AT 500 MEV - FINAL Leff - 0.005" Al 44" UPSTREAM of target

Space # 8: Distribution of particles as a function of X AT TGT2 (Element #169) (along HORIZONTAL axis)
& Y at TGT2 (Element #169) (along VERTICAL axis)

REAL! Distribution of FINAL RUN FOUND HERE

COUNTS = 149907.
X PROJECTION

Figure 4. The predicted beam spot at the target with scattering from the foil and 0.005 in.-thick aluminum window on an expanded scale.

97/11/18 - 2A AT 500 MEV - FINAL Leff - 0.005" Al 44", 0.010 Cu 16" UPSTREAM of target

Space # 9: Distribution of particles as a function of X AT TGT2 (Element #169) (along HORIZONTAL axis)
 & Y at TGT2 (Element #169) (along VERTICAL axis)

REAL! Distribution of FINAL RUN FOUND HERE

COUNTS = 149579.
 X PROJECTION

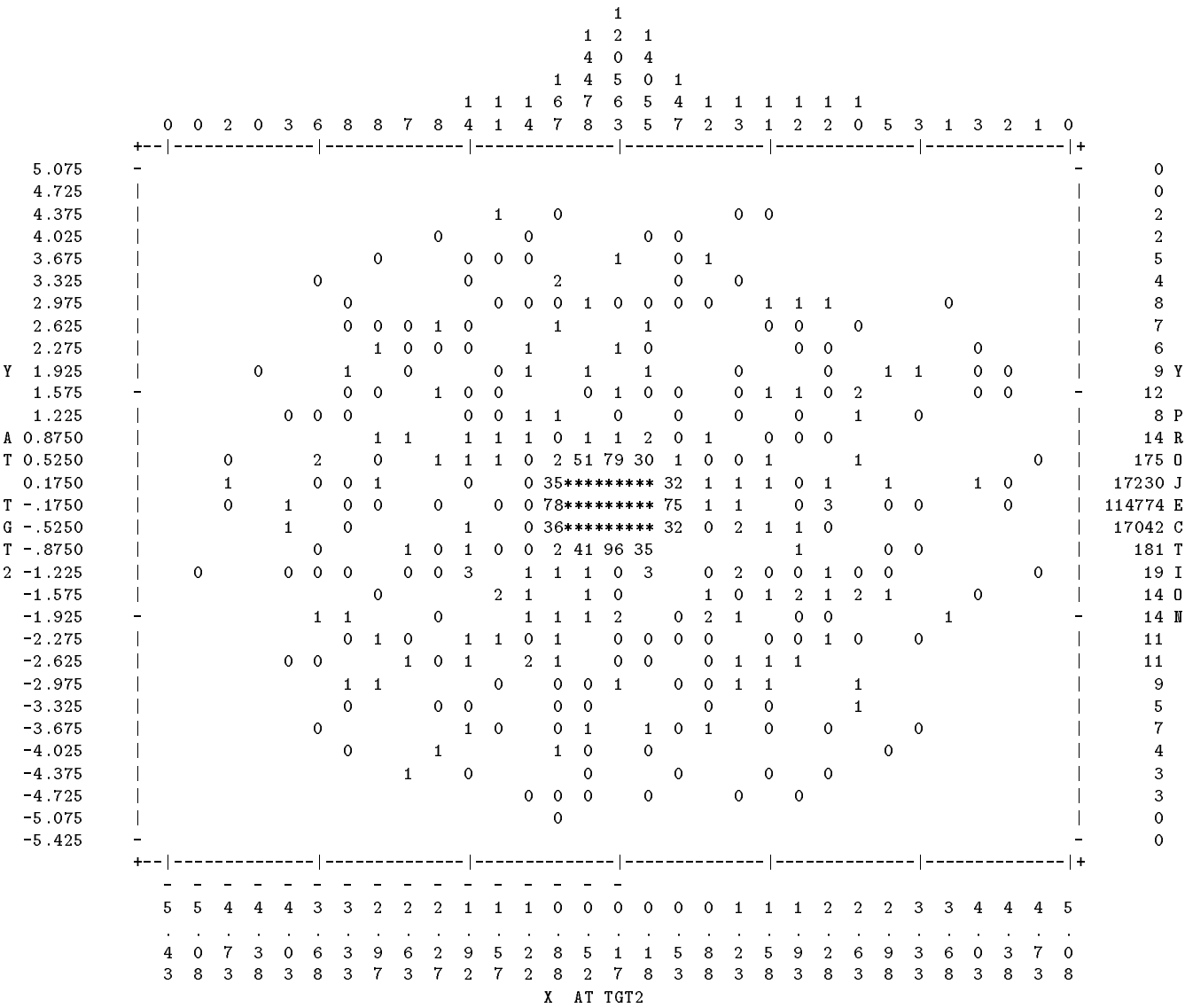


Figure 5. The predicted beam spot at the target with scattering from the foil and 0.005 in.-thick aluminum and 0.010 in.-thick copper windows.

97/11/18 - 2A AT 500 MEV - FINAL Leff - 0.005" Al 44", 0.010 Cu 16" UPSTREAM of target

Space # 7: Distribution of particles as a function of X AT TGT2 (Element #169) (along HORIZONTAL axis)
& Y at TGT2 (Element #169) (along VERTICAL axis)

REAL! Distribution of FINAL RUN FOUND HERE

COUNTS = 149579.
X PROJECTION

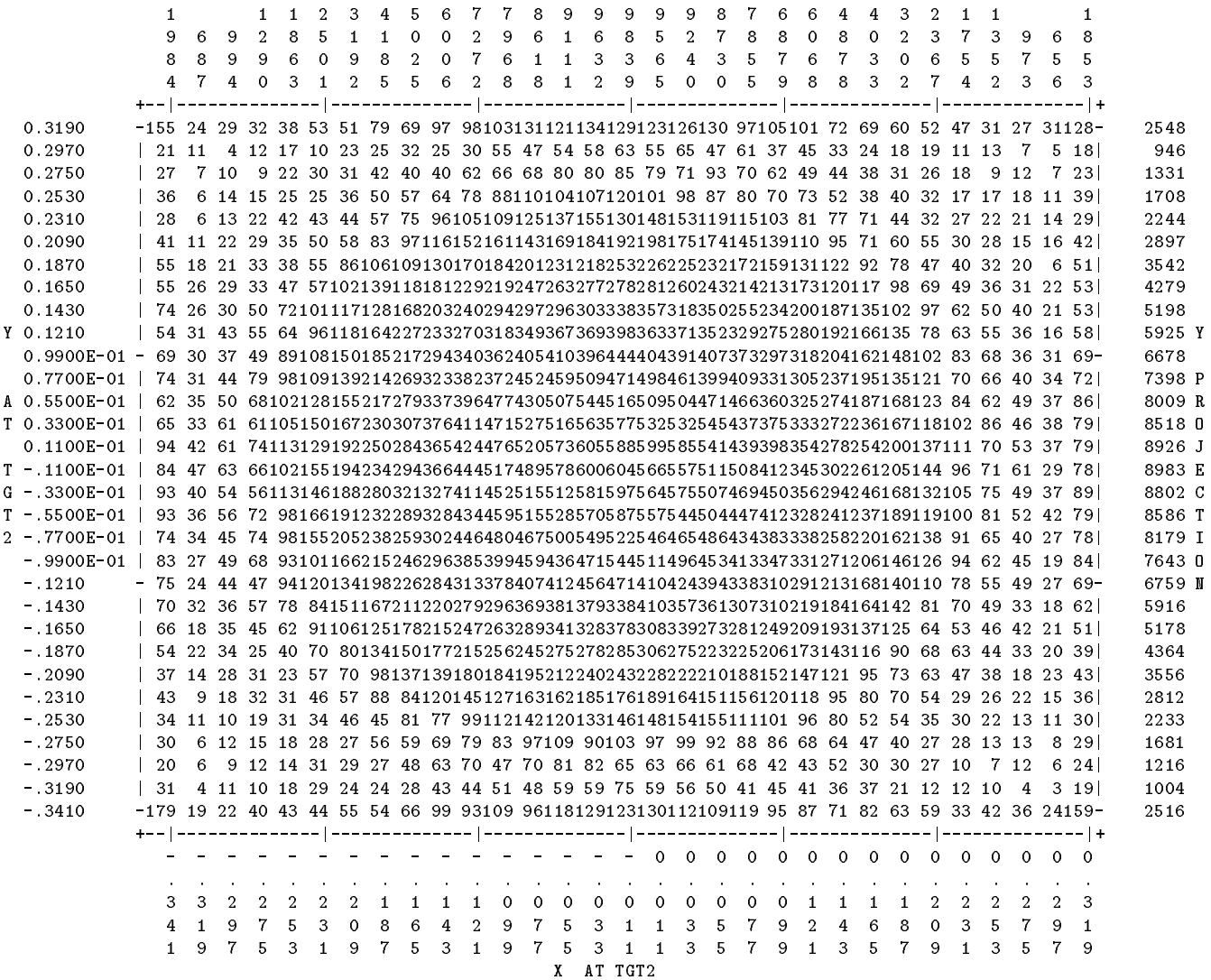
Figure 6. The predicted beam spot at the target with scattering from the foil and 0.005 in.-thick aluminum and 0.010 in.-thick copper windows on an expanded scale.

97/11/18 - 2A AT 500 MEV - FINAL Leff - 0.005" Al 44", 0.010 Cu 16" UPSTREAM of target

Space # 8: Distribution of particles as a function of X AT TGT2 (Element #169) (along HORIZONTAL axis)
 & Y at TGT2 (Element #169) (along VERTICAL axis)

REAL! Distribution of FINAL RUN FOUND HERE

COUNTS = 149579.
 X PROJECTION



97/11/18 - 2A AT 500 MEV - FINAL Leff - 0.005" Al 44", 0.010 Cu 16" UPSTREAM

Space # 1: Distribution of particles as a function of X AT ALW5 (Element #154) (along HORIZONTAL axis)
 & Y at ALW5 (Element #154) (along VERTICAL axis)

REAL! Distribution of FINAL RUN FOUND HERE

COUNTS = 149925.
 X PROJECTION

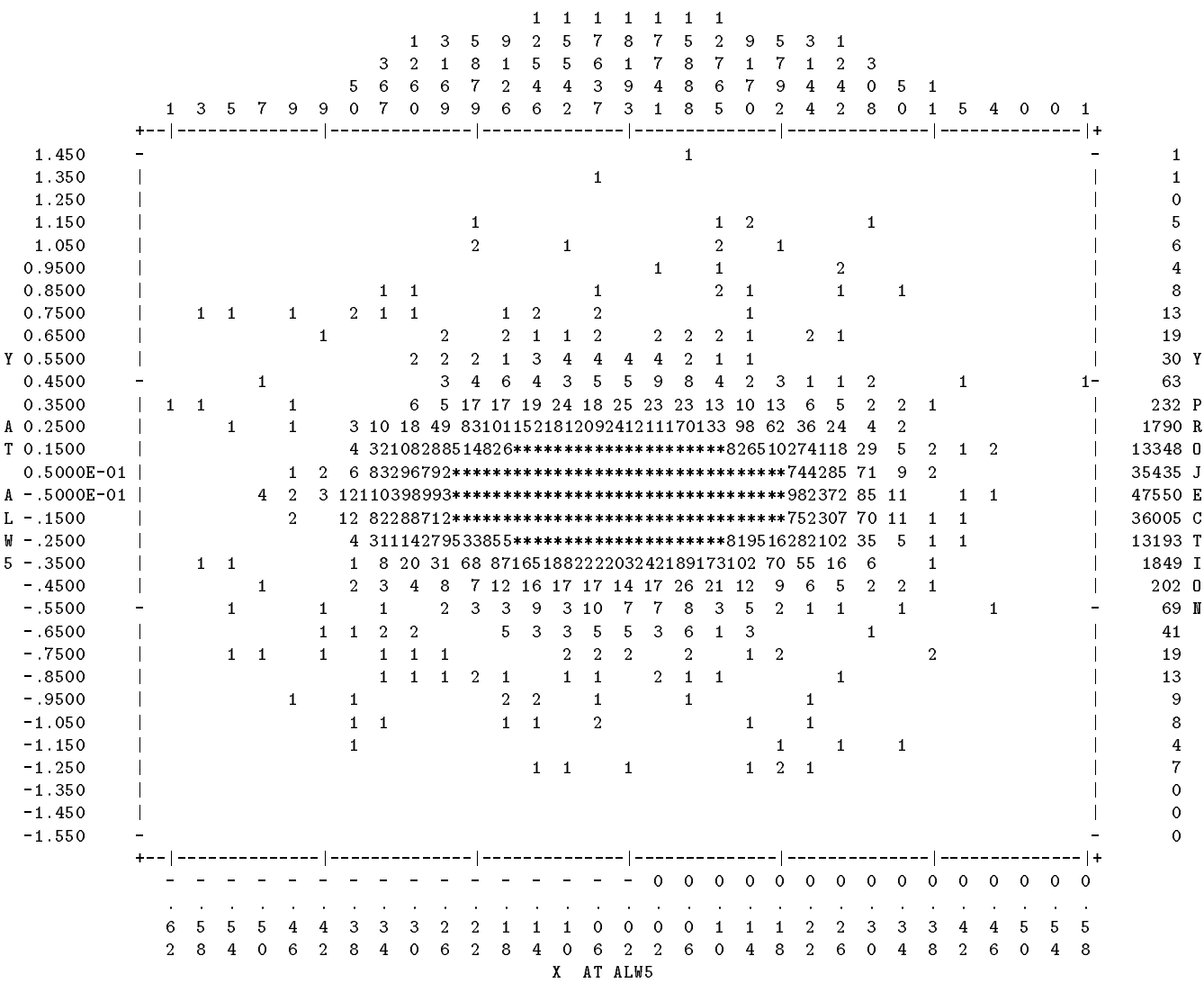


Figure 8. The predicted beam spot at the exit of the aluminum window.

97/11/18 - 2A AT 500 MEV - FINAL Leff - 0.005" Al 44", 0.010 Cu 16" UPSTREAM

Space # 2: Distribution of particles as a function of X AT M8382 (Element #155) (along HORIZONTAL axis)
 & Y at M8382 (Element #155) (along VERTICAL axis)

REAL! Distribution of FINAL RUN FOUND HERE

COUNTS = 149924.
 X PROJECTION

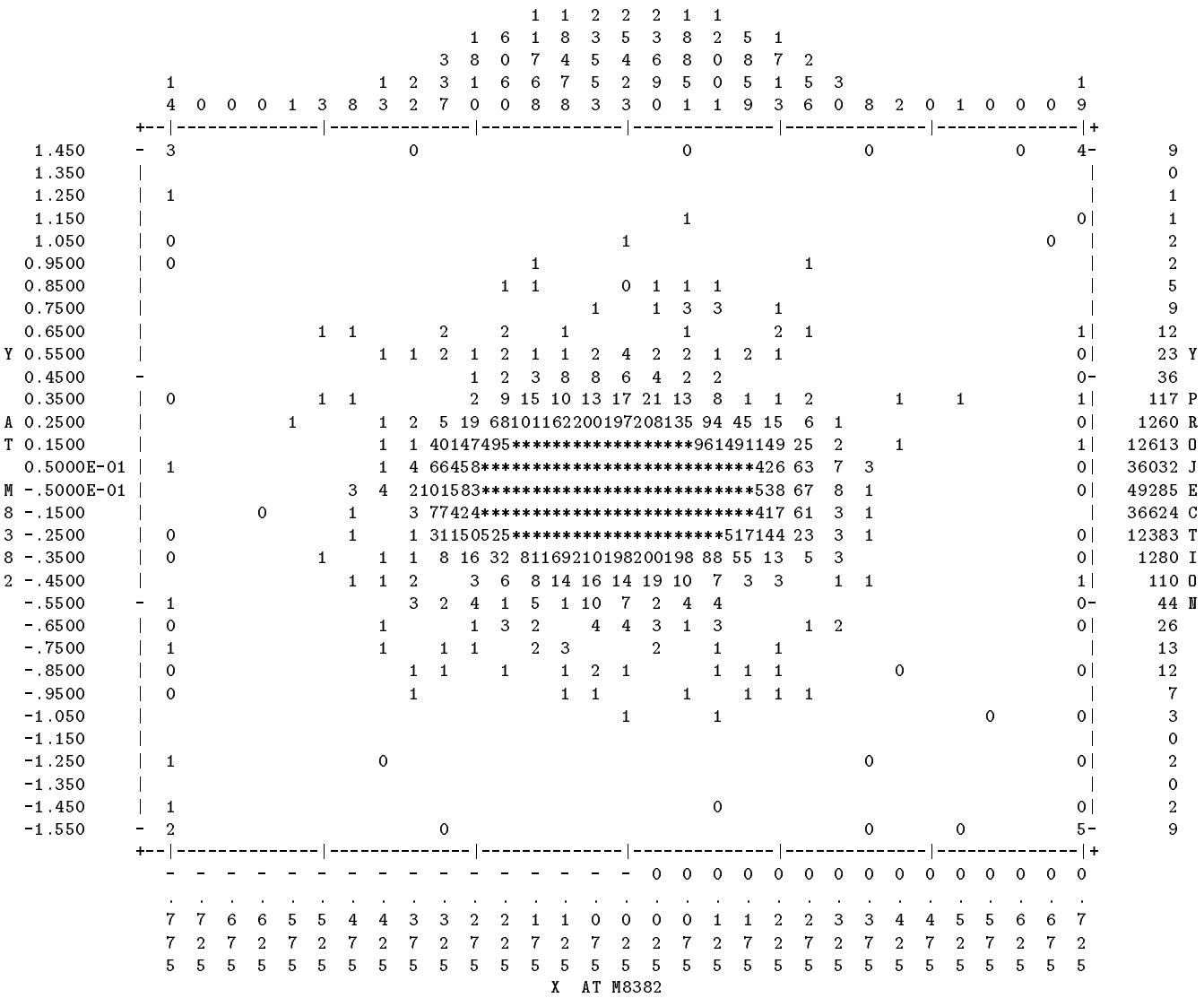


Figure 9. The predicted beam spot 0.2794 m (11 in.) downstream of the aluminum window.

97/11/18 - 2A AT 500 MEV - FINAL Leff = 0.005" Al 44", 0.010 Cu 16" UPSTREAM

Space # 3: Distribution of particles as a function of X AT M5588 (Element #156) (along HORIZONTAL axis)
& Y at M5588 (Element #156) (along VERTICAL axis)

REAL! Distribution of FINAL RUN FOUND HERE

COUNTS = 149904.
X PROJECTION

Figure 10. The predicted beam spot 0.5588 m (22 in.) downstream of the aluminum window.

97/11/18 - 2A AT 500 MEV - FINAL Leff - 0.005" Al 44", 0.010 Cu 16" UPSTREAM

Space # 4: Distribution of particles as a function of X AT M4064 (Element #157) (along HORIZONTAL axis)
 & Y at M4064 (Element #157) (along VERTICAL axis)

REAL! Distribution of FINAL RUN FOUND HERE

COUNTS = 149899.

X PROJECTION

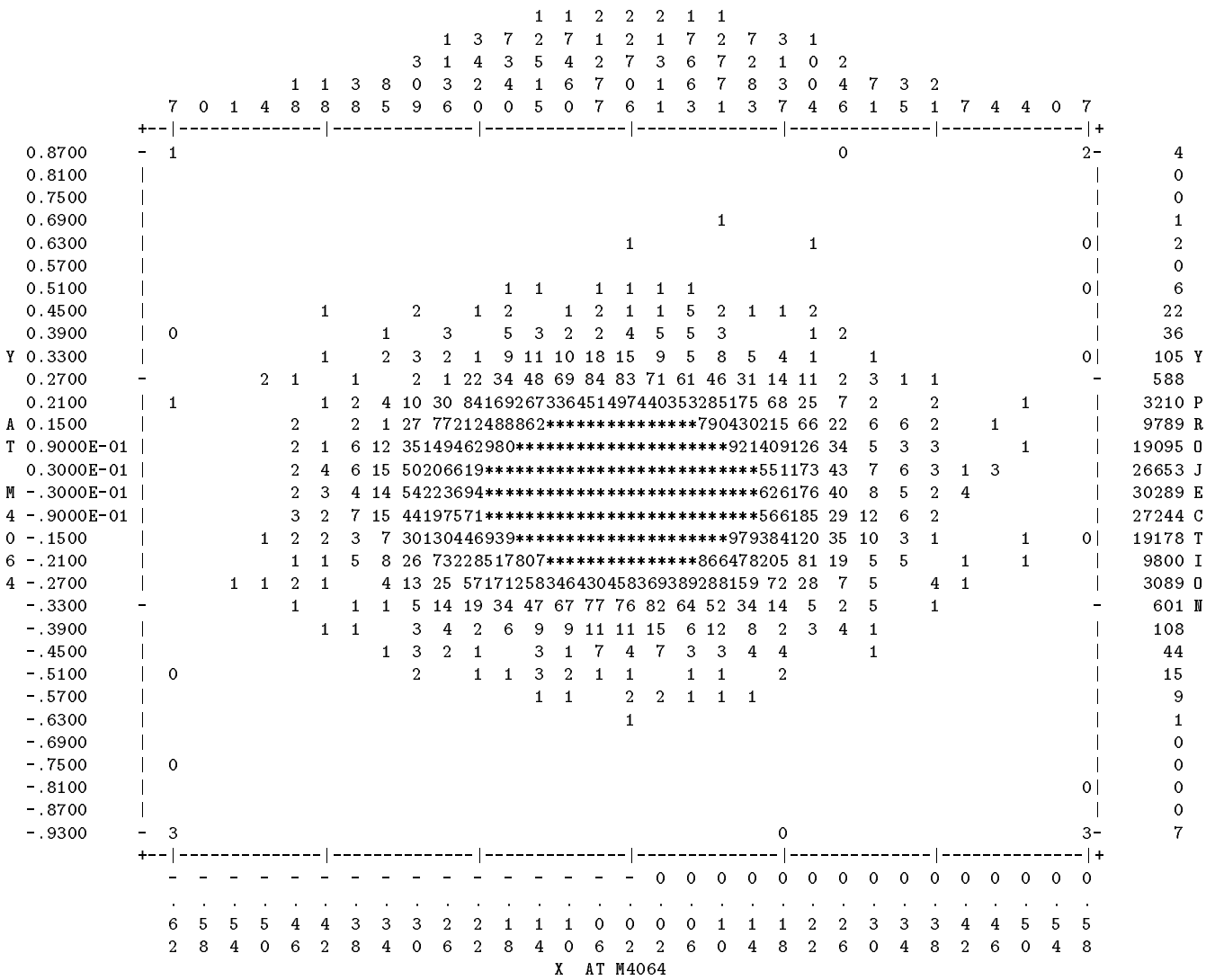


Figure 11. The predicted beam spot 0.7112 m (28 in.) downstream of the aluminum window.

97/11/18 - 2A AT 500 MEV - FINAL Leff = 0.005" Al 44", 0.010 Cu 16" UPSTREAM

Space # 7: Distribution of particles as a function of X AT M2794 (Element #168) (along HORIZONTAL axis)
& Y at M2794 (Element #168) (along VERTICAL axis)

REAL! Distribution of FINAL RUN FOUND HERE

COUNTS = 149611.

X PROJECTION

Figure 12. The predicted beam spot 0.1270 m (5 in.) downstream of the copper window and 0.2794 m (11 in.) upstream of the target.

97/11/18 - 2A AT 500 MEV - FINAL Leff = 0.005" Al 44", 0.010 Cu 16" UPSTREAM

Space # 2: Distribution of particles as a function of X AT ALW5 (Element #154) (along HORIZONTAL axis)
& Y at ALW5 (Element #154) (along VERTICAL axis)

REAL! Distribution of FINAL RUN FOUND HERE

COUNTS = 149925.
X PROJECTION

Figure 13. The predicted beam spot at the exit of the aluminum window on an enlarged scale.

97/11/18 - 2A AT 500 MEV - FINAL Leff - 0.005" Al 44", 0.010 Cu 16" UPSTREAM

Space # 7: Distribution of particles as a function of X AT CUW10 (Element #167) (along HORIZONTAL axis)
 & Y at CUW10 (Element #167) (along VERTICAL axis)

REAL! Distribution of FINAL RUN FOUND HERE

COUNTS = 149615.
 X PROJECTION

